Structure of Sputtered Amorphous Zr-Hf-Si Alloys

A. Pojtinger, P. Lamparter, and S. Steeb

Max-Planck-Institut für Metallforschung, Seestrasse 92, D-70174 Stuttgart, Germany

Reprint requests to Dr. P. L.; Fax: +49 711 2095420.

Z. Naturforsch. **54 a,** 699–703 (1999); received November 2, 1999

Amorphous $(Zr,Hf)_{37}Si_{63}$ alloys were produced by sputtering. Their total structure factors were determined by X-ray diffraction. Using the methods of isomorphous substitution and Reverse Monte Carlo simulation, the partial pair correlation functions were obtained. The results were compared with the partial functions of amorphous $Ti_{40}Si_{60}$. In the amorphous alloys under investigation the transition metal – metalloid correlation dominates the short range order.

Key words: Amorphous Zr-Hf-Si; X-ray Diffraction; RMC Model.

1. Introduction

The structure of binary amorphous alloys is described by three partial pair correlation functions. There are different ways to obtain the partial functions from diffraction experiments, such as the isotopic substitution technique [1], the combination of different kinds of radiation [2], a combination of X-ray and neutron diffraction by neglecting one of the three partial correlation functions [3], the method of isomorphous substitution [4] or computer simulations [5].

Amorphous transition metal – metalloid alloys can be formed by sputtering. In the present work the structure of sputtered amorphous $(Zr,Hf)_{37}Si_{63}$ alloys was investigated by X-ray diffraction. Zr and Hf are in the same column of the periodic table, and their Goldschmidt diameters D_{ij} of 3.20 Å and 3.18 Å, for Zr and Hf, respectively, are almost identical. This indicates that the chemical behaviour of Zr and Hf is very similar and that Zr and Hf can be substituted in amorphous alloys without affecting their structure [4, 6]. The much larger X-ray scattering length of Hf compared to that of Zr can be used to achieve a contrast variation by replacing Zr atoms by Hf atoms. For this purpose the three amorphous alloys $Zr_{37}Si_{63}$, $Hf_{18}Zr_{19}Si_{63}$ and $Hf_{37}Si_{63}$ were employed. The usual way to calculate directly the partial structure factors from three experimental total structure factors involves the problems given by the experimental errors in case of a weak contrast variation. As an alternative approach we used the Reverse Monte Carlo (RMC) method [7] to simulate the total structure factors. In this respect RMC can be regarded as a least squares method for the determination of partial structure factors from the experimental total structure factors. The results were compared with the partial functions of $Ti_{40}Si_{60}$ as derived in [5, 8].

2. Theoretical

According to Faber and Ziman [9] the total structure factor $S(Q)$ is obtained from the coherently scattered intensity per atom I_{coh}:

$$S(Q) = \frac{I_{\mathrm{coh}}(Q) - [\langle b^2\rangle - \langle b\rangle^2]}{\langle b\rangle^2}, \tag{1}$$

where $Q = (4\pi/\lambda)\sin\Theta$, 2Θ = scattering angle, λ = wavelength of the radiation, $\langle b\rangle = \sum_{i=1}^{n} c_i b_i$, $\langle b^2\rangle = \sum_{i=1}^{n} c_i b_i^2$, c_i = atomic concentration of the component i, b_i = coherent scattering length of the component i, n = number of components.

The total structure factor $S(Q)$ is a weighted sum of the partial structure factors $S_{ij}(Q)$:

$$\begin{aligned} S &= \frac{1}{\langle b\rangle^2}\sum_{i=1}^{n}\sum_{j=1}^{n} c_i c_j b_i b_j S_{ij}(Q) \\ &= \sum_{i=1}^{n}\sum_{j=1}^{n} W_{ij} S_{ij}(Q). \end{aligned} \tag{2}$$

From the partial structure factors $S_{ij}(Q)$ the partial pair correlation functions $G_{ij}(R)$ are obtained by Fourier transformation:

0932–0784 / 99 / 1200–0699 $ 06.00

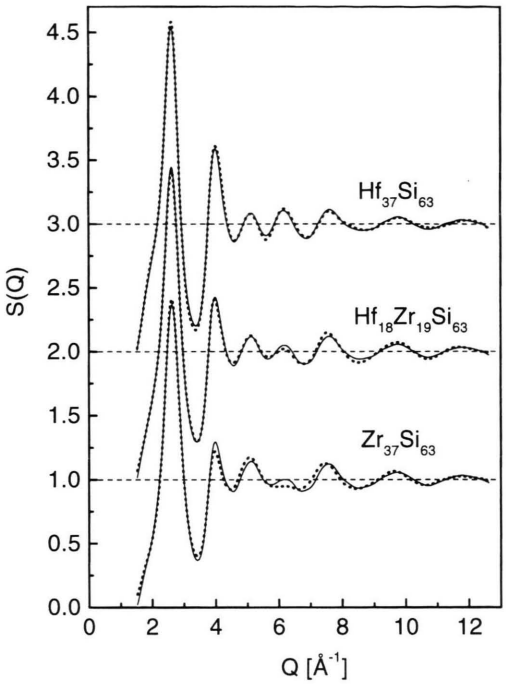

Fig. 1. Amorphous $Hf_{37}Si_{63}$, $Hf_{18}Zr_{19}Si_{63}$ and $Zr_{37}Si_{63}$: Total structure factors $S(Q)$. ··· from X-ray diffraction. — RMC-simulation.

$$G_{ij}(R) = \frac{2}{\pi}\int_0^\infty Q[S_{ij}^{FZ}(Q) - 1]\sin(QR)\mathrm{d}Q, \quad (3)$$

where R is the atomic distance.

The radial distribution function $\mathrm{RDF}_{ij}(R)$ can be written as

$$\mathrm{RDF}_{ij}(R) = c_j R\big(G_{ij}(R) + 4\pi\rho_0 R\big), \quad (4)$$

where ρ_0 is the number density.

The partial coordination number Z_{ij} is obtained from integration over the peak of the $\mathrm{RDF}_{ij}(R)$.

3. Experimental

3.1. Sample Preparation

The amorphous alloys $Zr_{37}Si_{63}$, $Hf_{18}Zr_{19}Si_{63}$ and $Hf_{37}Si_{63}$ were produced by sputtering as layers with a thickness between 20 µm and 30 µm. Mylar foil was used as substrate. The chemical composition of the samples was determined by electron microprobe and their densities were determined by X-ray grazing incidence reflectometry.

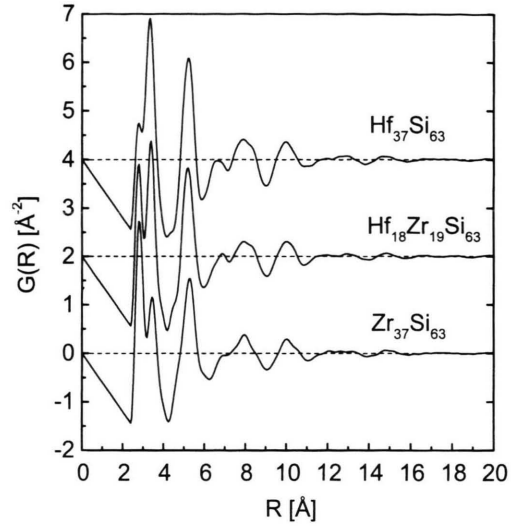

Fig. 2. Amorphous $Hf_{37}Si_{63}$, $Hf_{18}Zr_{19}Si_{63}$ and $Zr_{37}Si_{63}$: Total pair correlation functions $G(R)$ from X-ray diffraction.

3.2. X-ray Diffraction

The X-ray diffraction experiments were done with a diffractometer (Siemens D500) in transmission mode using Mo-K_α radiation. The measured intensities were corrected for Compton scattering [10, 11], polarisation [12] and absorption [11, 12]. In addition, the diffraction curves from the two samples containing Zr had to be corrected for fluorescence. The conversion into absolute scattering units and the calculation of the structure factors $S(Q)$ was done according to Krogh-Moe [13].

4. Results and Discussion

4.1. Total Structure Factors

The experimental structure factors $S(Q)$ are shown in Fig. 1 (dotted lines). The contrast variation caused by the substitution of Zr by Hf is particularly visible with the peaks no. 2, 3, and 4 which occur in the range $3.5\ \text{Å}^{-1} \leq Q \leq 7\ \text{Å}^{-1}$.

4.2. Total Pair Correlation Functions

Figure 2 shows the total pair correlation functions $G(R)$. The weighting factors W_{ij} of the partial pair correlation functions $G_{ij}(R)$ of the pseudobinary system $T_{37}Si_{63}$ (T = Hf, Zr) at $Q = 0$ are listed in Table 1. Together with the Goldschmidt diameters D_{ij} [14]

Table 1. Weighting factors W_{ij} (at $Q = 0$) for the partial correlation functions of $T_{37}Si_{63}$ alloys. T denotes the transition metals Zr and Hf.

$T_{37}Si_{63}$	W_{TT}	W_{TSi}	W_{SiSi}
$Zr_{37}Si_{63}$	0.393	0.468	0.139
$Hf_{18}Zr_{19}Si_{63}$	0.490	0.420	0.090
$Hf_{37}Si_{63}$	0.564	0.374	0.062

Table 2. Distances $D_{ij} = 0.5\ (D_i + D_j)$ of i-j pairs, where D_i, D_j are the Goldschmidt diameters [14].

	ZrZr	HfHf	ZrHf	SiSi	ZrSi	HfSi
D_{ij} [Å]	3.20	3.18	3.19	2.34	2.77	2.76

in Table 2, the total pair correlation functions can be interpreted. For all three alloys the first coordination shell is split into two peaks at $R^{I} \cong 2.8$ Å and $R^{II} \cong 3.3$ Å. For $Zr_{37}Si_{63}$ the first one is much higher than the second one, whereas the second one dominates for $Hf_{37}Si_{63}$. For $Hf_{18}Zr_{19}Si_{63}$ the amplitudes of both peaks are between the amplitudes of the $Hf_{37}Si_{63}$ and $Zr_{37}Si_{63}$ peaks. Comparing the R-values of both peaks inside the first coordination shell with the diameters D_{ij} in Table 2, it is suggested that the first peak at R^{I} is mainly generated by the metal-metalloid correlation T-Si. The decrease of the amplitude of this peak from $Zr_{37}Si_{63}$ via $Hf_{18}Zr_{19}Si_{63}$ to $Hf_{37}Si_{63}$ is in line with the decrease of the weighting factor W_{TSi} of the T-Si correlation. The second peak at R^{II} inside the first coordination shell arises from the metal-metal correlation T-T. Its amplitude increases in the same way as the weighting factor W_{TT} for $Zr_{37}Si_{63}$ via $Hf_{18}Zr_{19}Si_{63}$ to $Hf_{37}Si_{63}$. The atomic distances R^{I} and R^{II} in the amorphous alloys are slightly larger than the corresponding Goldschmidt diameters in Table 2.

4.3. Partial Pair Correlation Functions

Using the RMC method, a three-dimensional atomic cluster was obtained. As a guideline for the simulations the experimental total structure factors were used. For the number density ρ_0 of the three alloys the value 0.0530 Å^{-3} was used, which was determined by X-ray reflectometry. As a starting configuration for the RMC run, a random cluster of 1500 atoms was taken. After $5 \cdot 10^6$ accepted atomic displacements good agreement with the three measured $S(Q)$ could be obtained, as shown in Figure 1. From this atomic cluster the partial pair correlation functions $G_{ij}(R)$, shown in Fig. 3a), were determined. The structural parameters are listed in Table 3. The atomic distances R_{ij} and the widths σ_{ij} were taken from the first peak of the $G_{ij}(R)$ functions. The partial coordination numbers Z_{ij} were obtained from Gaussian fitting to the peaks of the $RDF_{ij}(R)$ functions. The results in Fig. 3a) show that the RMC method is capable to resolve the peaks of the Si-Si and the T-Si correlations which do not appear separately in the first peak at R^{I} of the experimental $G(R)$ functions. The Si-Si distance $R_{SiSi} = 2.63$ Å is distinctly larger than the Goldschmidt diameter $D_{SiSi} = 2.34$ Å. Also the atomic distance $R_{TT} = 3.36$ Å is larger than the corresponding Goldschmidt diameters D_{ij} ($D_{HfHf} = 3.18$ Å, $D_{ZrZr} = 3.20$ Å).

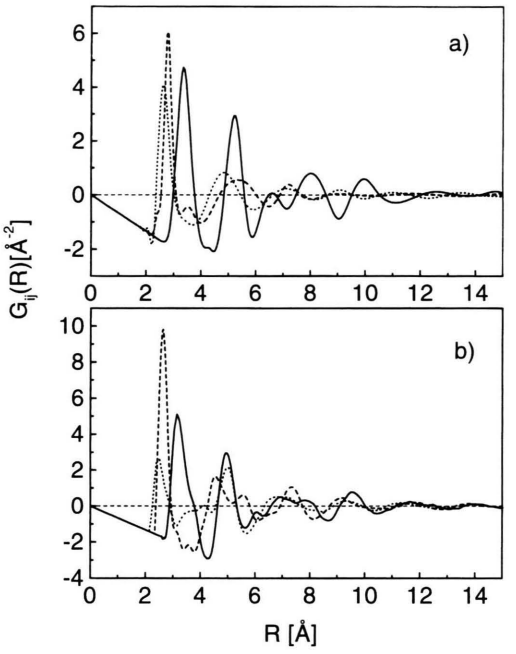

Fig. 3. Partial pair correlation functions $G_{ij}(R)$. a) amorphous $(Hf,Zr)_{37}Si_{63}$, from RMC-simulation. b) amorphous $Ti_{40}Si_{60}$ [5, 8]. — metal-metal, - - - metal-Si, ··· Si-Si.

Table 3. Amorphous $(Zr,Hf)_{37}Si_{63}$: atomic distances R_{ij}, widths σ_{ij} of the first peaks of the pair distribution and partial coordination numbers Z_{ij}. T = transition metal (Zr, Hf).

	TT	TSi	SiT	SiSi
R_{ij} [Å]	3.36	2.78	–	2.63
σ_{ij} [Å]	0.50	0.26	–	0.35
Z_{ij}	5.6	5.9	3.5	5.9

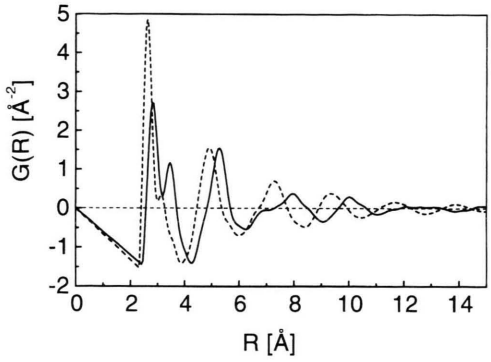

Fig. 4. Total pair correlation functions $G(R)$. — $Zr_{37}Si_{63}$, - - - $Ti_{40}Si_{60}$ [5, 8].

The partial correlation function $G_{TSi}(R)$ in Fig. 3a) shows a sharp first peak with a width of 0.26 Å which is distinctly smaller than the widths of the metal-metal correlation and of the metalloid-metalloid correlation. The atomic distance R_{TSi} = 2.78 Å agrees well with the Goldschmidt diameters D_{HfSi} = 2.76 Å and D_{ZrSi} = 2.77 Å, but it is smaller than the average of the distances R_{SiSi} and R_{TT} by about 7%. In addition, the T-Si peak is distinctly sharper than the T-T peak. These features reflect the chemical bonding between the metal atoms and the metalloid atoms.

The results indicate that the T-Si correlation dominates the chemical short range order. Consequently the T-T and the Si-Si correlations have to accomodate in some way to the T-Si correlation which leads to distances larger than the Goldschmidt diameters and to broader peaks.

4.4. Amorphous $(Zr,Hf)_{37}Si_{63}$ Compared with Amorphous $Ti_{40}Si_{60}$

It is interesting to investigate whether the preceding results are valid only for amorphous (Zr,Hf)-Si alloys or for other amorphous transition metal – metalloid alloys, too. In this chapter the structural accords and differences between $(Zr,Hf)_{37}Si_{63}$ and $Ti_{40}Si_{60}$ will be discussed. Ti belongs to the same column of the periodic table as Hf and Zr. Thus the chemical behaviour is similar. However, the Goldschmidt diameter is smaller for Ti (D_{TiTi} = 2.91 Å) than for Zr and Hf (Table 2). The different sizes of the transition metal atoms certainly influences the structures of the amorphous alloys.

Figure 4 shows the total pair correlation function $G(R)$ of $Zr_{37}Si_{63}$ compared with that of $Ti_{40}Si_{60}$ [8]. The partial pair correlation functions $G_{ij}(R)$ of $Ti_{40}Si_{60}$ [5] are shown in Figure 3b). In Table 4 the weighting factors W_{ij} for X-rays (at Q = 0), the atomic distances R_{ij}, the width σ_{ij} of the first peaks, and the partial coordination numbers Z_{ij} are listed for $Ti_{40}Si_{60}$. The total pair correlation functions $G(R)$ of $Ti_{40}Si_{60}$ and $Zr_{37}Si_{63}$ exhibit two peaks in the first coordination shell. For $Ti_{40}Si_{60}$ the height of the first peak with respect to the height of the second peak is larger than for $Zr_{37}Si_{63}$. Furthermore, for $Zr_{37}Si_{63}$ the peaks of the function $G(R)$ are shifted to larger R-values compared with $Ti_{40}Si_{60}$. The first effect is partly to be expected because the ratio W_{TiSi}/W_{TiTi} is larger than the ratio W_{ZrSi}/W_{ZrZr}. The shift of the peaks is due to the different sizes of the Ti and the Zr atoms. The partial pair correlation functions $G_{ij}(R)$ in Fig. 3a) and b) and the structural parameters in Table 3 and Table 4 yield more detailed information about the differences and accords of the amorphous alloys $Ti_{40}Si_{60}$ and $Zr_{37}Si_{63}$. For both alloys the metalloid – metalloid correlations and the transition metal – transition metal correlations are wider than the transition metal – metalloid correlation and the atomic distances are larger than the corresponding Goldschmidt diameters. This indicates that also for amorphous $Ti_{40}Si_{60}$ the transition metal – metalloid correlation dominates the chemical short range order. Furthermore, it is remarkable that for both alloys the transition metal – transition metal correlation in the second coordination shell is marked. Only the Si-Si correlation of the two alloys is quite different. The Si-Si distance in $Zr_{37}Si_{63}$ is 2.63 Å, whereas in $Ti_{40}Si_{60}$ it is 2.48 Å, and the coordination number in $Zr_{37}Si_{63}$ is Z_{SiSi} = 5.9, whereas in $Ti_{40}Si_{60}$ it is Z_{SiSi} = 3.6. Probably, this difference is due to the larger size of the Zr and Hf atoms.

Table 4. Amorphous $Ti_{40}Si_{60}$: weighting factors W_{ij} (at Q = 0), atomic distances R_{ij}, widths σ_{ij} of the first peaks of the pair distribution, and partial coordination numbers Z_{ij} [5, 8].

	TiTi	TiSi	SiTi	SiSi
W_{ij}	0.262	0.500	–	0.239
R_{ij} [Å]	3.14	2.64	–	2.48
σ_{ij} [Å]	0.66	0.31	–	0.43
Z_{ij}	6.6	6.8	4.5	3.6

5. Conclusions

The structure of amorphous $(Zr,Hf)_{37}Si_{63}$ was investigated by X-ray diffraction. From isomorphous

substitution of Zr and Hf a contrast variation was achieved. Using the Reverse Monte Carlo simulation method, the partial pair correlation functions were obtained. These functions indicate that the (Hf,Zr)-Si correlation dominates the chemical short range order (CRSO). The amorphous $(Zr,Hf)_{37}Si_{63}$ alloys were compared with amorphous $Ti_{40}Si_{60}$. For the $Ti_{40}Si_{60}$ alloy the transition metal - metalloid correlation dominates the CRSO, too. Thus the transition metal - metalloid interaction is the driving force and responsible for the structure of the investigated alloys. The differences between the partial pair correlation functions of $(Zr,Hf)_{37}Si_{63}$ and $Ti_{40}Si_{60}$, respectively, are due to the different sizes of the transition metal atoms.

[1] P. Lamparter and S. Steeb, in: Materials Science and Technology, Vol. 1, Chapt. 4, ed. V. Gerold, VCH, Weinheim 1993, p. 217.
[2] J. Ankele, Doctor thesis, University of Stuttgart 1998.
[3] P. Lamparter, A. Habenschuss, and A. H. Narten, J. Non-Cryst. Sol. **86**, 109 (1986).
[4] C. N. J. Wagner and D. Lee, J. Phys. **C8**, 242 (1980).
[5] A. Pojtinger, R. Bellissent, P. Lamparter, and S. Steeb, Z. Naturforsch. **50a**, 749 (1995).
[6] D. Chipman, L. Jennings, and B. C. Giessen, Bull. Amer. Phys. Soc. **23**, 467 (1978).
[7] R. L. McGreevy and L. Pusztai, Mol. Simulation **1**, 359 (1988).
[8] A. Pojtinger, Doctor thesis, University of Stuttgart 1994.
[9] T. E. Faber and J. M. Ziman, Phil. Mag. **11**, 153 (1965).
[10] J. H. Hubell, Wm. J. Veigele, E. A. Briggs, R. T. Brown, D. T. Cromer, and R. J. Howerton, J. Phys. Chem. Ref. Data **4**, 2130 (1975).
[11] K. Sagel, Tabellen zur Röntgenstrukturanalyse, Springer-Verlag, Berlin 1950.
[12] C. N. J. Wagner, J. Non-Cryst. Sol. **31**, 1 (1978).
[13] J. Krogh-Moe, Acta Cryst. **9**, 951 (1956).
[14] W. Hume Rothery and G. V. Raynor, The Structure of Metals and Alloys, 3rd ed., Inst. of Metals, London 1954.